

White dwarf-main sequence binaries from SDSS DR 8: unveiling the cool white dwarf population

A. Rebassa-Mansergas^{1,2}, C. Agurto-Gangas², M. R. Schreiber^{2,3}, B.T. Gänsicke⁴,
D. Koester⁵

¹ *Kavli Institute for Astronomy and Astrophysics, Peking University, Beijing 100871, China*

² *Departamento de Física y Astronomía, Universidad de Valparaíso, Avenida Gran Bretaña 1111, Valparaíso, Chile*

³ *Millennium Nucleus "Protoplanetary Disks in ALMA Early Science," Universidad de Valparaíso, Avenida Gran Bretaña 1111, Valparaíso, Chile*

⁴ *Department of Physics, University of Warwick, Coventry CV4 7AL, UK*

⁵ *Institut für Theoretische Physik und Astrophysik, University of Kiel, 24098 Kiel, Germany*

Accepted 2013. Received 2013; in original form 2013

ABSTRACT

The spectroscopic catalogue of white dwarf-main sequence (WDMS) binaries from the Sloan Digital Sky Survey (SDSS) is the largest and most homogeneous sample of compact binary stars currently known. However, because of selection effects, the current sample is strongly biased against systems containing cool white dwarfs and/or early type companions, which are predicted to dominate the intrinsic population. In this study we present colour selection criteria that combines optical (*ugriz* DR 8 SDSS) plus infrared (*yjhz* DR 9 UKIRT Infrared Sky Survey (UKIDSS), *JHK* Two Micron All Sky Survey (2MASS) and/or *w₁w₂* Wide-Field Infrared Survey Explorer (WISE)) magnitudes to select 3 419 photometric candidates of harboring cool white dwarfs and/or dominant (M dwarf) companions. We demonstrate that 84 per cent of our selected candidates are very likely genuine WDMS binaries, and that the white dwarf effective temperatures and secondary star spectral types of 71 per cent of our selected sources are expected to be below $\lesssim 10\,000$ – $15\,000$ K, and concentrated at $\sim M2$ – 3 , respectively. We also present an updated version of the spectroscopic SDSS WDMS binary catalogue, which incorporates 47 new systems from SDSS DR 8. The bulk of the DR 8 spectroscopy is made up of main-sequence stars and red giants that were targeted as part of the Sloan Extension for Galactic Understanding and Exploration (SEGUE) Survey, therefore the number of new spectroscopic WDMS binaries in DR 8 is very small compared to previous SDSS data releases. Despite their low number, DR 8 WDMS binaries are found to be dominated by systems containing cool white dwarfs and therefore represent an important addition to the spectroscopic sample. The updated SDSS DR 8 spectroscopic catalogue of WDMS binaries consists of 2316 systems. We compare our updated catalogue with recently published lists of WDMS binaries and conclude that it currently represents the largest, most homogeneous and cleanest sample of spectroscopic WDMS binaries from SDSS.

Key words: (stars:) binaries (including multiple): close – stars: low-mass – (stars): white dwarfs – (stars:) binaries: spectroscopic.

1 INTRODUCTION

White dwarf-main sequence binaries (WDMS) are compact binary stars that descend from main sequence binaries, and are among the most common compact binary objects in the Galaxy. The majority (~ 75 per cent) of the initial main sequence binaries from which WDMS binaries derive have orbital separations wide enough to avoid mass transfer interactions. Therefore the primary (or more massive) main

sequence star evolves as a single star and the orbital separation widens as a result of the primary losing mass at the asymptotic giant branch (Willems & Kolb 2004). In the remaining (~ 25 per cent) of the cases the main sequence stars are close enough for mass transfer to be initiated via Roche-lobe overflow once the primary ascends the red giant branch or the the asymptotic giant branch. Unstable mass transfer to the secondary main sequence companion generally brings the system into a common envelope phase (CE;

Iben & Livio 1993; Webbink 2008), in which the orbital separation dramatically decreases due to drag forces of the binary components with the material of the envelope, formed by the outer layers of the giant. The energy released due to the shrinkage of the orbit is used to expel the envelope (Davis et al. 2010; Zorotovic et al. 2010; Ricker & Taam 2012; Passy et al. 2012; Rebassa-Mansergas et al. 2012b), exposing a post-CE binary (PCEB) composed of the core of the giant, i.e. the future white dwarf, and the secondary main sequence companion. The orbital period distribution of WDMS binaries is therefore bimodal, with the close PCEBs peaking at short orbital periods of ~ 8 hours (Miszalski et al. 2009; Nebot Gómez-Morán et al. 2011) and the systems that did not evolve through a CE phase at much wider orbital separations (orbital periods > 100 days, Willems & Kolb 2004; Farihi et al. 2010).

After the envelope is ejected, PCEBs continue to evolve to even shorter orbital periods through angular momentum loss driven by magnetic braking and/or gravitational wave emission. Therefore PCEBs may either undergo a second phase of CE evolution (leading to double-degenerate white dwarfs), or enter a semi-detached state (and appear as cataclysmic variables or super-soft X-ray sources).

Thanks to the Sloan Digital Sky Survey (SDSS, York et al. 2000; Stoughton et al. 2002) the number of WDMS binaries has increased from a few ten (Schreiber & Gänsicke 2003) to over two thousand (Silvestri et al. 2006; Heller et al. 2009; Morgan et al. 2012; Liu et al. 2012; Wei et al. 2013). The latest version of our WDMS binary catalogue (Rebassa-Mansergas et al. 2012a), based on SDSS data release (DR) 7, contains 2248 systems, and represents the most complete and homogeneous sample. Follow-up observational studies based on this large sample have led to the identification of a large number of wide binaries and close PCEBs (e.g. Rebassa-Mansergas et al. 2007; Schreiber et al. 2008, 2010) that are being used to study several different and important aspects in modern astrophysics (e.g. providing crucial constraints on current theories of CE evolution (Davis et al. 2010; Zorotovic et al. 2010; Rebassa-Mansergas et al. 2012b) and on the origin of low-mass white dwarfs (Rebassa-Mansergas et al. 2011); testing theoretical mass-radius relations of both white dwarfs and low-mass main sequence stars (Nebot Gómez-Morán et al. 2009; Pyrzas et al. 2009, 2012; Parsons et al. 2010, 2012a,b); and constraining the pairing properties of main sequence stars (Ferrario 2012)).

The currently known population of SDSS WDMS binaries is formed by systems observed as part of the first and second phases of the operation of SDSS: SDSS-I and SDSS-II. Whilst SDSS-I focused on targeting galaxies and quasars (Adelman-McCarthy et al. 2008), SDSS-II carried out three different surveys (Abazajian et al. 2009): the Sloan Legacy Survey that completed the original SDSS-I imaging and spectroscopic goals; the SEGUE survey (the SDSS Extension for Galactic Understanding and Exploration, Yanny et al. 2009), that obtained additional imaging over a large range of Galactic latitudes as well as spectroscopy for $\sim 240\,000$ stars; and the Sloan Supernova Survey that carried out repeat imaging of the 300 square degree southern equatorial stripe to discover and measure supernovae and other variable objects.

Due to the overlap between the colours of WDMS binaries containing hot white dwarfs and/or late-type (M dwarf) companions and those of quasars (Smolčić et al. 2004), the target selection algorithm of both SDSS-I and the Legacy Survey of SDSS-II resulted in a large number of WDMS binaries with available SDSS spectroscopy. SEGUE additionally performed a dedicated survey for finding WDMS binaries containing cool white dwarfs and/or early-type M dwarfs/late-type K dwarfs based on colour selection criteria developed by our team (Schreiber et al. 2007; Rebassa-Mansergas et al. 2012a). However, despite the success of our SEGUE survey, the 251 systems identified in this way represent only ~ 10 per cent of the known population of SDSS WDMS binaries, hence remain still clearly under-represented. Moreover, it is important to bear in mind that any WDMS binary sample based on optical colours/spectra alone, such as the SDSS sample, is bound to be incomplete as only binaries with both components visible at optical wavelengths can be identified.

The aim of this paper is to build on the spectroscopic SDSS WDMS binary catalogue by identifying WDMS binaries within the photometric footprint of SDSS DR 8 without the need of SDSS spectra, and to extend the parameter range of the known WDMS binary population by extending the wavelength range used for their identification, thus overcoming the selection effects just described. For this purpose, we develop colour selection criteria based on a combination of SDSS optical plus infrared magnitudes for selecting WDMS binaries, specifically focused on detecting systems containing cool white dwarfs and/or companions dominating the system luminosity, which are predicted to represent a large fraction of the intrinsic population (Schreiber & Gänsicke 2003). In addition, we search for new spectroscopic WDMS binaries observed by DR 8.

2 THE PHOTOMETRIC SELECTION

We select photometric WDMS binary candidates following a two-step procedure. First, we apply colour selection criteria based on SDSS *ugriz* magnitudes, which allows us to exclude single main-sequence stars. Second, we search for available infrared excess detections of our selected candidates and apply additional colour cuts based on a combination of optical plus infrared magnitudes. This efficiently excludes quasars from our candidate list and selects WDMS binaries dominated by the flux of the secondary star, i.e. systems that contain cool white dwarfs and/or early-type (M dwarf) main sequence companions.

2.1 Photometric selection of WDMS binaries in SDSS

SDSS WDMS binaries form a “bridge” in colour space that connects the white dwarf locus to that of low-mass stars (Smolčić et al. 2004). Based on this bridge we develop the following colour criteria for selecting WDMS binaries within SDSS:

$$15 \leq g \leq 19, \quad (1)$$

$$(u - g) > -0.6, \quad (2)$$

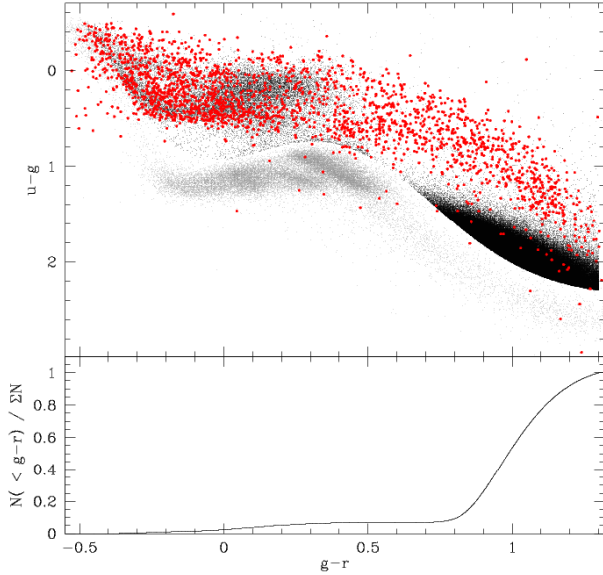


Figure 1. Top panel: photometrically selected SDSS WDMS binary candidates in the $u - g$ vs. $g - r$ plane (black solid dots). Spectroscopically confirmed SDSS WDMS binaries from Rebassa-Mansergas et al. (2012a) are shown as red solid dots and main sequence stars as gray solid dots. Bottom panel: $g - r$ cumulative distribution of the photometrically selected candidates.

$$-0.5 < (g - r) < 1.3, \quad (3)$$

$$-0.4 < (r - i) < 1.6, \quad (4)$$

$$-0.8 < (i - z) < 1.15 \quad (5)$$

$$(u - g) < 0.93 - 0.27 \times (g - r) - 4.7 \times (g - r)^2 + 12.38 \times (g - r)^3 + 3.08 \times (g - r)^4 - 22.19 \times (g - r)^5 + 16.67 \times (g - r)^6 - 3.89 \times (g - r)^7 \quad (6)$$

$$(g - r) < 2 \times (r - i) + 0.38 \quad \text{if} \quad -0.4 < (r - i) \leq 0.06 \quad (7)$$

$$(g - r) < 0.5 \quad \text{if} \quad 0.06 < (r - i) \leq 0.3 \quad (8)$$

$$(g - r) < 4.5 \times (r - i) - 0.85 \quad \text{if} \quad 0.3 < (r - i) \leq 0.48 \quad (9)$$

$$(r - i) < 0.5 + (i - z) \quad \text{if} \quad (i - z) \leq 0 \quad (10)$$

$$(r - i) < 0.5 + 2 \times (i - z) \quad \text{if} \quad (i - z) > 0 \quad (11)$$

We use the *casjobs* interface (Li & Thakar 2008)¹ to select the number of point sources with clean photometry and magnitude errors below 0.1 within the photometric data base of SDSS DR 8, satisfying our colour selection. This search results in 953 835 WDMS binary candidates (see Table 1), illustrated as black solid dots in the $u - g$ vs. $g - r$ plane (top panel of Figure 1). For comparison, we show also main sequence stars (gray solid dots) and the 2248 spectroscopically confirmed WDMS binaries from SDSS DR 7 (red solid dots, Rebassa-Mansergas et al. 2012a). In the bottom

Table 1. The number of photometrically selected WDMS binary candidates as function of the progressively refined colour selections. The colour cut in each step is described in more detail in the main text. The final number of WDMS binary photometric selected candidates is 3 419.

NWDMS	description	excludes
953 835	SDSS colours	main sequence stars
67 378	refined SDSS colours	galaxies
48 163	IR detections	objects with no IR
4 237	optical plus infrared colours	quasars
3 419	comparison with WD catalogues	white dwarfs

panel of Figure 1 we represent the $g - r$ cumulative distribution of our 953 835 selected sources.

A close inspection of the bottom panel of Figure 1 reveals that $g - r > 0.6$ for $\gtrsim 90$ per cent of our WDMS binary candidates. These systems are concentrated near the main sequence star locus (see top panel of Figure 1), and overlap only with ~ 3 per cent of the spectroscopically confirmed WDMS binaries. Inspection of SDSS spectra of objects falling within this colour space reveals ~ 98 per cent of these systems being galaxies². We therefore decide to refine our selection criteria to exclude these objects from our sample and re-write Equation 6 as follows:

$$(u - g) < 0.93 - 0.27 \times (g - r) - 4.7 \times (g - r)^2 + 12.38 \times (g - r)^3 + 3.08 \times (g - r)^4 - 22.19 \times (g - r)^5 + 16.67 \times (g - r)^6 - 3.89 \times (g - r)^7 \quad \text{if} \quad (g - r) \leq 0.52, \quad (12)$$

$$(u - g) < 0.4 + (g - r) \quad \text{if} \quad (g - r) > 0.52 \quad (13)$$

Our refined selection criteria are shown on the top panels of Figure 2 (black solid lines) and reduce the number of photometrically selected WDMS binary candidates to 67 378 (see Table 1). For comparison, main sequence stars (gray solid dots), quasars (green solid dots) and spectroscopically confirmed SDSS WDMS binaries (red solid dots) are also shown. From Figure 2 (top panels) it is apparent that single main sequence stars are efficiently excluded with our colour selection. However, our sample is expected to be highly contaminated by quasars. Single white dwarfs are also expected to be a large source of contamination, as white dwarf colours are similar to those of WDMS binaries in which the white dwarf flux dominates the spectral energy distribution.

2.2 Infrared excess

Here we search for available infrared excess detections of our 67 378 selected candidates (Table 1) and develop additional selection criteria based on a combination of optical plus infrared magnitudes that allow us to efficiently exclude quasars. We do this by cross-correlating our list with the *yjhk* UKIDSS DR 9 (Lawrence et al. 2007; Warren et al. 2007), *JHK* 2MASS (Skrutskie et al. 2006) and *w₁w₂* WISE

² It is intriguing that such a relatively large number of galaxies were flagged by SDSS as point-sources, thus passing our initial selection criteria.

¹ <http://skyserver.sdss3.sdss.org/CasJobs/>

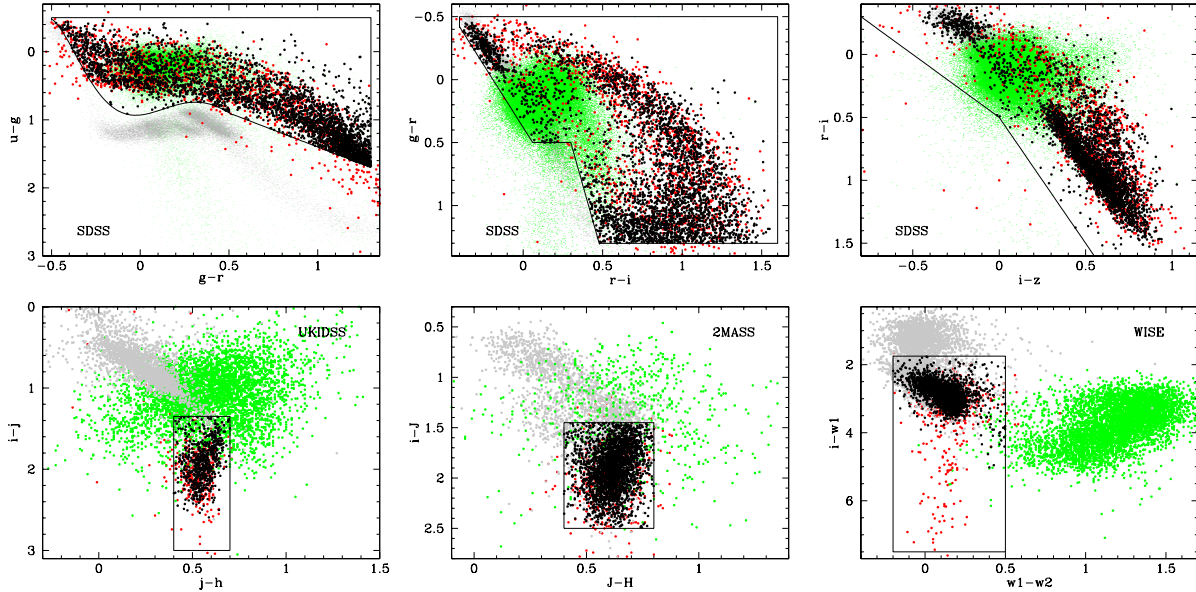


Figure 2. Colour selection of WDMS binaries that combines optical SDSS and infrared UKIDSS, 2MASS and/or WISE magnitudes (black solid lines) and the 3 419 resulting photometric WDMS binary selected candidates (black solid dots). To illustrate how main sequence stars and quasars are efficiently excluded with our selection criteria we represent a sample of quasars from Schneider et al. (2010) as solid green dots and main sequence stars as gray solid dots. Spectroscopically confirmed SDSS WDMS binaries from Rebassa-Mansergas et al. (2012a) are also shown as red solid dots.

(Wright et al. 2010) surveys. In all cases we restrict the search to the best quality data, i.e. we use quality flags AAA in 2MASS and AA in WISE. This results in 48 163 objects with available detections in at least one of the three considered infrared surveys (Table 1). We further consider only objects satisfying the following conditions:

$$1.35 < (i - j) < 3, \quad 0.4 < (j - h) < 0.7 \quad (14)$$

$$1.45 < (i - J) < 2.5, \quad 0.4 < (J - H) < 0.8 \quad (15)$$

$$1.75 < (i - w_1) < 7.5, \quad -0.2 < (w_1 - w_2) < 0.5 \quad (16)$$

The above colour criteria are illustrated on the bottom panels of Figure 2 (black solid lines) and reduce the list of photometric WDMS binary candidates to 4 237 (Table 1). Inspection of Figure 2 (bottom panels) reveals that quasars are indeed efficiently excluded by our selection criteria.

2.3 Comparison with white dwarf catalogues

As mentioned above, single white dwarfs are also expected to be an important source of contamination in our sample. Fortunately, comprehensive catalogues of single white dwarfs within the SDSS DR7 footprint are available (Girven et al. 2011; Debes et al. 2011; Kleinman et al. 2013). We compare our WDMS binary candidate list with the catalogues of Kleinman et al. (2013) and Girven et al. (2011) and exclude all positive matches. This reduces our number of selected candidates to 3 419 (Table 1), shown as black solid dots in Figure 2. Coordinates, optical SDSS and infrared UKIDSS,

2MASS and WISE magnitudes of the 3 419 photometrically selected WDMS binaries can be found in Table 2³.

It is worth mentioning that the photometric white dwarf catalogue of Girven et al. (2011) includes SDSS white dwarfs for which UKIDSS near-infrared excess is detected, which implies we might be excluding some genuine WDMS binaries in this exercise. However, the overlap between our WDMS binary photometric candidate list and the sample of WDMS binaries that may be included in the catalogue by Girven et al. (2011) is very small, as the colour selection by Girven et al. (2011) removes any white dwarf that has a noticeable excess in the SDSS i magnitude, i.e. the main interest of that study is to detect infrared excess typical of debris discs around or brown dwarf companions to white dwarfs. It is also important to keep in mind that the single white dwarf catalogues are based on SDSS DR 7 and that we are considering DR 8 data here. Therefore, a few per cent of single white dwarfs may still be included in our WDMS binary candidate list.

2.4 The success rate of the photometric sample

We have demonstrated that our selection criteria are highly efficient in excluding single main sequence stars and quasars. Single white dwarfs have also been eliminated from our list. However, the remaining WDMS binary candidate sample may contain a small number of other astronomical objects with similar colours such as e.g. cataclysmic variables. It

³ Among the 3 419 selected candidates, 1 109 have available $yjhk$ UKIDSS magnitudes, 2 459 available JHK 2MASS magnitudes, 2 606 available w_1w_2 WISE magnitudes, and 501 available magnitudes from all three infrared surveys.

Table 2. Object names, coordinates (in degrees) and SDSS *ugriz*, UKIDSS *yjkhk*, 2MASS *JHK* and WISE *w₁w₂* magnitudes of the 3419 photometrically selected WDMs binaries. For those with available spectroscopy, we include the spectral classification (Table 3). The complete table is available in the electronic edition of the paper.

SDSS J	ra	dec	<i>u</i>	<i>g</i>	<i>r</i>	<i>i</i>	<i>z</i>	<i>y</i>	<i>j</i>	<i>h</i>	<i>k</i>	<i>J</i>	<i>H</i>	<i>K</i>	<i>w₁</i>	<i>w₂</i>	type
000116.50+000204.8	0.31874	0.03468	18.85	18.80	18.91	19.04	19.22	18.90	18.94	0.00	0.00	0.00	0.00	0.00	0.00	0.00	unknown
000152.09+000644.5	0.46703	0.11236	19.03	18.57	17.89	17.48	17.17	16.51	16.05	15.40	15.28	0.00	0.00	0.00	0.00	0.00	WDMs
000218.67-064850.1	0.57781	-6.81391	20.44	18.96	17.78	17.19	16.79	0.00	0.00	0.00	0.00	15.65	14.93	14.74	14.66	14.73	-
000238.16+162756.7	0.65898	16.46576	19.13	18.56	17.84	16.80	16.13	0.00	0.00	0.00	0.00	14.76	14.16	13.89	13.79	13.68	-
000356.94-050332.8	0.98723	-5.05910	18.53	18.22	18.15	17.48	16.88	0.00	0.00	0.00	0.00	15.58	14.98	14.50	14.48	14.42	WDMs
000413.91+183616.4	1.05795	18.60455	18.71	18.53	18.57	17.87	17.23	0.00	0.00	0.00	0.00	15.84	15.16	14.96	14.79	14.61	-
000504.91+243409.6	1.27047	24.56934	19.51	18.89	18.47	17.48	16.81	0.00	0.00	0.00	0.00	15.36	14.72	14.40	14.26	14.11	WDMs
000541.94+133734.2	1.42474	13.62616	19.23	18.77	18.86	19.05	19.17	18.87	18.99	0.00	0.00	0.00	0.00	0.00	0.00	0.00	-
000553.76+113128.5	1.47402	11.52457	18.84	18.83	19.00	19.23	19.46	19.13	19.20	0.00	0.00	0.00	0.00	0.00	0.00	0.00	-
000559.88-054416.1	1.49948	-5.73780	18.56	18.32	17.75	17.06	16.62	0.00	0.00	0.00	0.00	15.43	14.84	14.73	14.43	14.40	WDMs

Table 3. Classification of 567 WDMs binary candidates in our list from available SDSS spectroscopy. The large percentage of genuine WDMs binaries indicates a high success rate of our colour criteria in selecting WDMs binaries.

Type	N	percentage
WDMs	468	82.5
CV	21	3.7
MS	16	2.8
MS+MS sup.	2	0.3
QSO	46	8.1
extinction MS	2	0.3
unknown	12	2.4

is therefore important to evaluate the success rate in identifying WDMs binaries among our photometric candidates (hereafter success rate). We do this as follows.

From our list of 3 419 photometrically selected WDMs binary candidates (Table 1), 567 have SDSS spectroscopy which we visually classify as follows (Table 3): 468 WDMs binaries, 21 cataclysmic variables, 16 main sequence stars, 2 main sequence-main sequence star superpositions, 46 quasars, 2 main sequence stars heavily affected by extinction and 12 objects of unknown type. The large number of WDMs binaries in the spectroscopic sample indicates a high success rate (~ 83 per cent, Table 3). Apparently, a small number of quasars that passed our cuts, together with some cataclysmic variables are the main sources of contamination.

It is to be expected that, depending on the colour space, the success rate varies, i.e. that the ~ 83 per cent we obtained represents an average success rate over the entire colour space. In order to evaluate this hypothesis we divide the *u-g* vs. *g-r*, *g-r* vs. *r-i* and *r-i* vs. *i-z* planes into cells of 0.15. Within each cell we calculate the local success rate as $N_{\text{wdms}}/N_{\text{spec}}$, where N_{wdms} and N_{spec} are the number of spectroscopic WDMs binaries and the number of systems with available spectroscopy respectively. The dependence of the success rate on location in colour space is illustrated in Figure 3. If we take into account only cells with $N_{\text{spec}} > 20$, the minimum and maximum success rate we obtain are 43 per cent and 100 per cent respectively (Figure 3). It is also evident that the success rate increases towards redder objects.

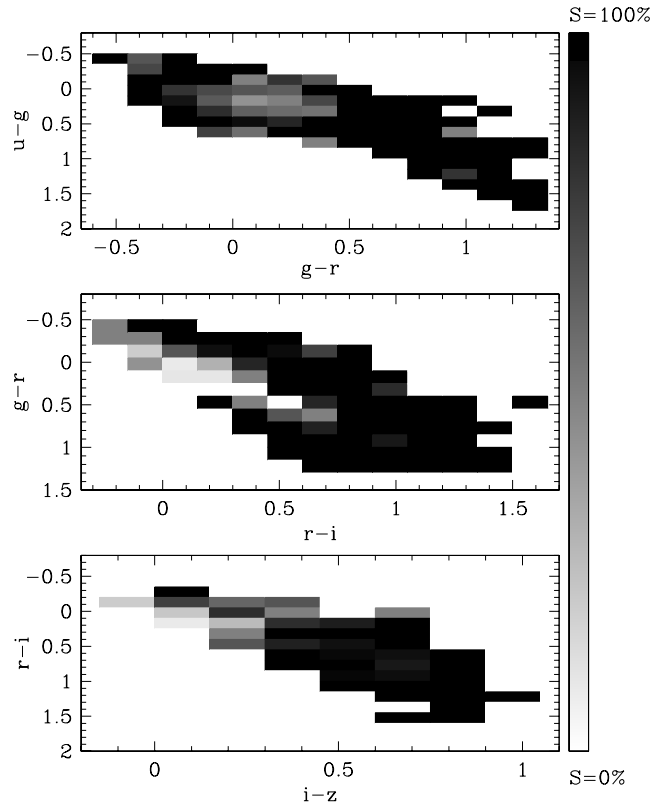


Figure 3. Density maps that represent the success rate (*S*) in selecting WDMs binaries by our colour criteria in the *u-g* vs. *g-r* (top panel), *g-r* vs. *r-i* (middle panel) and *r-i* vs. *i-z* (bottom panel) planes.

2.5 Characterization of the photometric sample

Here we investigate the stellar properties of our photometric WDMs binary candidate sample. The top panel of Figure 4 shows the distribution of the 3 419 selected sources (Table 1) as a function of *u-g*. We calculate, for the same binning as for the *u-g* distribution, the average (and standard deviation) white dwarf effective temperatures and secondary star spectral types of the spectroscopically confirmed SDSS WDMs binaries from Rebassa-Mansergas et al. (2012a),

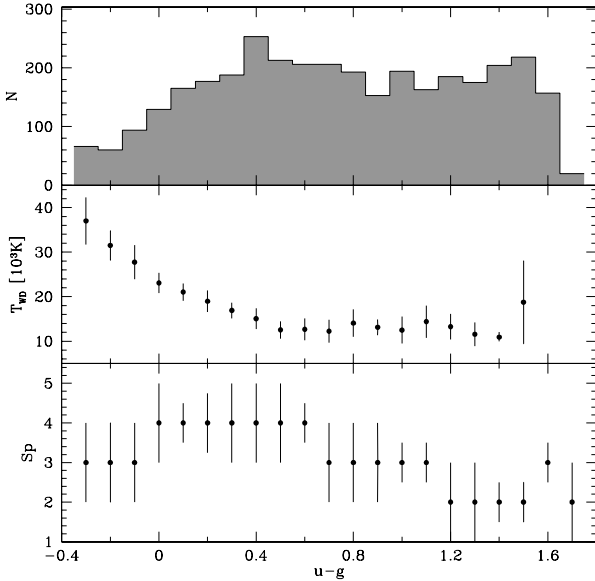


Figure 4. Top panel: distribution of the 3419 photometric SDSS WDMS binary candidates (Table 1) as a function of $u-g$. Middle and bottom panels: average white dwarf effective temperatures and secondary star (M dwarf) spectral sub-types of spectroscopically confirmed SDSS WDMS binaries also as a function of $u-g$. The majority of our selected photometric candidates are expected to be WDMS binaries with dominant M dwarfs and/or cool white dwarfs.

and represent the obtained values on the middle and bottom panels of Figure 4 respectively.

The white dwarf effective temperatures show a clear decrease with increasing $u-g$, followed by a flat distribution at $\sim 10\,000$ – $15\,000$ K for $u-g \gtrsim 0.4$. For values of $u-g > 1.3$, the spectroscopic fits do not provide reliable values for the white dwarf effective temperatures either because the white dwarfs are extremely cool and/or because the flux of the M dwarf dominates the spectral energy distribution in the SDSS spectra. The spectral types of the secondary stars are of $\sim M3$ – 4 for a broad range of $u-g$ and show a trend towards earlier spectral types ($\sim M2$) for $u-g > 1.2$.

This analysis clearly demonstrates that our colour criteria selects mainly (~ 70 per cent) WDMS binaries dominated by the flux of the secondary star and/or containing cool white dwarfs ($\sim M2$ – 3 , $T_{\text{eff}} \lesssim 10\,000$ – $15\,000$ K), a population that is under-represented in the current spectroscopic sample of SDSS WDMS binaries.

3 THE SPECTROSCOPIC CATALOGUE

Our analysis of the spectroscopic DR7 resulted in the identification of 2248 WDMS binaries (Rebassa-Mansergas et al. 2012a). Here, we test both if our photometric selection (Section 2) identifies WDMS binaries that we missed in our spectroscopic classification of DR7, and if there are any new spectroscopic WDMS binaries in DR8. We first cross-correlate the 468 systems in our photometric sample that have available SDSS spectra (Table 3) with the 2248 confirmed WDMS binaries from DR7, and incorporate all pos-

sible missing objects to the list. We then follow the methods outlined by Rebassa-Mansergas et al. (2010) to search for additional spectroscopic WDMS binaries within DR8.

3.1 Comparison with the photometric sample

19 WDMS binaries with available SDSS spectra from our photometric sample (Section 2) are not included in the list by Rebassa-Mansergas et al. (2012a). Of these, seven are part of DR8 and are therefore new additions to the catalogue: SDSSJ082845.07+133551.0, SDSSJ093011.64+095319.5, SDSSJ101356.32+272410.6, SDSSJ102122.45+433633.1, SDSSJ102627.48+384502.4, SDSSJ121150.94+110543.2, SDSSJ145722.85-012121.2).

The remaining 12 systems are from DR7 and are divided into:

- five M dwarf dominated WDMS binaries (SDSSJ014113.10-084831.0, SDSSJ083833.17+140332.1, SDSSJ151251.47+010201.2, SDSSJ212125.32+010541.6, SDSSJ235143.39+362736.6).
- six apparently single M dwarfs with strong Balmer emission lines due to a (likely) close white dwarf that heats the surface of the M dwarf and/or due to magnetic activity (Tappert et al. 2011; Rebassa-Mansergas et al. 2013) (SDSSJ054251.34+010206.8, SDSSJ074645.01+425327.4, SDSSJ080239.07+102026.0, SDSSJ090210.97+252913.5, SDSSJ093127.22+151855.0, SDSSJ102804.59+081321.9).
- one G star plus (hot) white dwarf (SDSSJ142838.99+424024.8).

In all 12 cases the SDSS spectra do not reveal strong white dwarf features, which explains why these systems were missed by Rebassa-Mansergas et al. (2012a). The addition of the 19 systems to the spectroscopic SDSS WDMS binary catalogue raises the number of spectroscopic SDSS WDMS binaries to 2267 (Table 4).

3.2 The template-fitting method

Here we identify new DR8 SDSS WDMS binaries following the routine developed by Rebassa-Mansergas et al. (2010). This technique is based on reduced χ^2 template fitting all new DR8 spectra, as well as on signal-to-noise (S/N) ratio constraints. The template set consists of 163 spectra of previously confirmed SDSS WDMS binaries covering a broad range of white dwarf effective temperatures and spectral subtypes (DA, DB and DC) as well as companion star spectral types (M0–M9). In practice, an equation of the form

$$\chi_{\text{max}}^2 = a \times (S/N_{\text{spec}})^b \quad (17)$$

is defined for each of the 163 templates, where χ_{max}^2 is the maximum χ^2 allowed between the template and the considered SDSS spectrum, S/N_{spec} is the signal-to-noise ratio of the SDSS spectrum, and a and b are fixed values that vary from template to template. All objects falling below the curve defined for each template are considered WDMS binary candidates. In the process of WDMS binary search we inspect the available SDSS DR8 images of the selected candidates in order to detect morphological problems. This can be the case when single white dwarfs or M dwarfs are located close to very bright stars that cause scattered light

Table 4. New spectroscopic SDSS WDMS binaries have been identified in this work through different methods, outlined in Section 3 and summarised in this table. In the last column we provide the section to refer to for further details.

method	candidate WDMS	QSO	M dwarf	WDMS	DR 8 WDMS	total WDMS	total DR 8 WDMS	
comparison with phot. sample	-	-	-	19	7	2267	7	Section 3.1
χ^2 -SN fitting	2353	18	456	44	37	2297	37	Section 3.2
M dwarf+GALEX; blue excess	456	-	-	8	8	2305	45	Section 3.3
completeness analysis	2001	942	11	38	38	2306	46	Section 3.4
M dwarf+GALEX; blue excess	11	-	-	0	0	2306	46	
literature review	-	-	-	3	0	2309	46	Section 3.5
catalogue review	-	-	-	-2,+1	0	2308	46	
comparison with Liu et al. (2012)	28	-	-	0	0	2308	46	Section 3.5
comparison with Morgan et al. (2012)	85	-	-	5	1	2313	47	
comparison with Wei et al. (2013)	281	-	-	3	0	2316	47	

to enter the spectroscopic fibre and result in an apparent two-component spectrum; other cases can be the superposition along the line of sight between two stars. All these objects are removed from our candidate list.

We obtain a list of 2353 WDMS binary candidates and visual inspection of the spectra of these candidates results in 44 genuine WDMS binaries (Table 4). Of the 44 identified systems, seven objects are included in the list of DR 7 WDMS binaries by Rebassa-Mansergas et al. (2012a), therefore only 37 are new additions (these include the seven WDMS binaries identified in Section 3.1). The majority of the rejected candidates are early type main sequence stars plus a noticeable fraction of M dwarfs (456, see Table 4). We identify only 18 quasar spectra and no spectra with white dwarf features. The sample of 456 M dwarfs is further investigated in the next section, as a fraction of these might be WDMS binaries containing cool/unseen white dwarfs.

The relatively small number of WDMS binaries with spectroscopy found within DR 8, compared to earlier data releases, is a direct consequence of the spectroscopic DR 8 being dominated by single main sequence stars and giants that were observed as part of SEGUE (Aihara et al. 2011; Eisenstein et al. 2011).

3.3 Identification of blue excess

Searching for WDMS binaries within the spectroscopic DR 8 we have identified 456 apparently single M dwarfs (Table 4). These may be genuine M dwarfs or WDMS binaries containing very cool and/or unseen white dwarfs. We here follow two procedures for identifying white dwarf primaries that contribute very little to the optical flux of the binaries.

First, we cross-correlate our list of 456 M dwarf selected spectra with the near- and far-ultraviolet magnitudes provided by the Galaxy Evolution Explorer (GALEX DR 6, Martin et al. 2005; Morrissey et al. 2005; Seibert et al. 2012). A clear excess in the near or far-ultraviolet GALEX fluxes confirms the presence of a white dwarf primary that contributes too little to be unambiguously detected at optical wavelengths. An example is shown on the bottom panel of Figure 5.

An additional way of identifying cool and/or unseen white dwarf primaries is by searching for blue excess in the

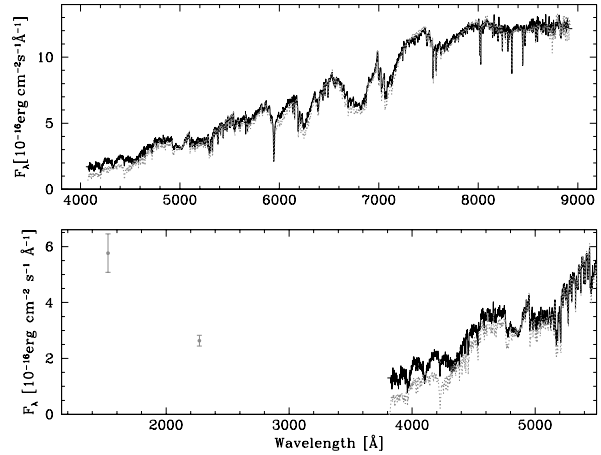


Figure 5. SDSS spectrum of SDSSJ 011004.70+071702.8, an M dwarf dominated WDMS binary. The presence of a white dwarf is confirmed by template fitting the spectrum with an M2 template (top panel, gray dotted line) and by the GALEX near- and far-ultraviolet detections (bottom panel, gray solid dots).

M dwarf dominated spectra. We do this by fitting the spectra with the M0 to M9 templates of Rebassa-Mansergas et al. (2007). We calculate the reduced χ^2 between the M dwarf spectra and the best-fit template over the 4000-5000 Å (χ_b^2) and the 7000-9000 Å (χ_r^2) wavelength ranges. Objects with $\chi_b^2/\chi_r^2 > 2$ are selected as WDMS binaries containing unseen white dwarfs. However, as shown by Rebassa-Mansergas et al. (2010), this method is likely to provide false detections in case of low signal-to-noise ratio spectra, and is prone to select active M dwarfs. We therefore visually inspect the spectra of all blue excess candidates. An example of a WDMS binary recovered in this way is shown on the top panel of Figure 5.

The search for blue excess and positive detections in GALEX DR 6 confirms the presence of white dwarf primaries in eight systems among the 456 single M dwarf candidate spectra, thus increasing the total number of spectroscopic WDMS binaries to 2305 (Table 4).

3.4 Catalogue completeness

We evaluate here the internal completeness of the new SDSS DR8 spectroscopic sample of WDMS binaries, i.e. the fraction of all WDMS binaries contained in the DR8 spectroscopic data base that we have identified. In Rebassa-Mansergas et al. (2010, 2012a) we approached this aim by analysing small areas in colour space that are representative of the SDSS WDMS binary population. Here we base our study on the entire WDMS binary bridge (Smolčić et al. 2004). This is motivated by the fact that the bulk of the DR8 spectroscopy is made up of single main sequence and giant stars obtained as part of SEGUE that can be easily excluded applying the colour selection criteria defined by Equations 1-11.

We use the *casjobs* interface to detect the number of point sources with clean photometry and available DR8 SDSS spectra that satisfy Equations 1-11. Note that in this exercise we restrict the search for spectroscopic sources that form part *only* of the new data released by DR8. This search results in 2001 WDMS binary candidates (Table 4). Visual inspection of the 2001 candidate spectra reveals 38 WDMS binaries, 942 quasars and 11 M dwarfs that might be genuine M stars or WDMS binaries containing cool and/or unseen white dwarf primaries (Table 4, the majority of the remaining spectra are main sequence stars affected by extinction, main sequence-main sequence star superpositions, and some early type main sequence stars). Among the 11 M dwarf spectra, none are confirmed as WDMS binaries due to blue excess detected in the spectrum or as resulting from positive GALEX DR 6 detections.

All WDMS binaries identified in this exercise except one (SDSSJ155847.38+431308.4, an M dwarf dominated WDMS binary) are included in our DR8 WDMS binary list, thus providing a completeness of ~ 98 per cent. We add SDSSJ155847.38+431308.4 to our catalogue and the number of spectroscopically confirmed SDSS WDMS binaries thus raises to 2306.

4 THE FINAL SPECTROSCOPIC SDSS DR8 WDMS BINARY CATALOGUE

In this work we have raised the number of spectroscopic SDSS WDMS binaries to 2306 (Table 4). To this list we include the recently discovered WDMS binaries SDSSJ013851.54-001621.6 (Parsons et al. 2012b, which contains an ultra-cool white dwarf), SDSSJ135523.92+085645.4 (Badenes et al. 2013, which contains a hot white dwarf and a likely brown dwarf companion) and SDSSJ013532.97+144555.9 (Steele et al. 2013, which contains a brown dwarf companion). In these three cases, the SDSS spectra are totally dominated by one of the stellar components, making it very difficult for our template fitting routine to identify these systems as WDMS binaries. In addition, we include SDSSJ053317.31-004321.9, a resolved K star plus white dwarf binary that we previously missed. Finally, we exclude from our catalogue SDSSJ014349.22+002130.0, for which the blue excess detected by Rebassa-Mansergas et al. (2010) is likely to come from a nearby quasar rather than a white dwarf, and SDSSJ144335.19+004005.9, which is an eclipsing binary

containing two M dwarfs with an orbital period of ~ 1 day (S.G. Parsons, private communication). This brings the total number of spectroscopic SDSS WDMS binaries to 2308 (Table 4).

In the course of writing this paper three sets of SDSS WDMS binaries have been published by three different groups (Liu et al. 2012; Morgan et al. 2012; Wei et al. 2013), and we compare our set of 2308 systems with these three samples in what follows.

4.1 Comparison with Liu et al. (2012)

We detect all 523 WDMS binaries from Liu et al. (2012) except for 28 systems that we do not consider WDMS binaries after a visual inspection of the SDSS spectra. An updated classification for these systems is given in Table A1.

4.2 Comparison with Morgan et al. (2012)

A comparison with the 1756 systems of Morgan et al. (2012) reveals that we are missing 85 objects. Inspecting the SDSS spectra and images of these 85 systems we classify 80 as non-WDMS binaries (Table A2). The remaining five systems are:

- SDSSJ000421.61+004341.5, a DR 7 noisy spectrum of a M star plus some blue excess.
- SDSSJ083833.17+140332.1, an M dwarf dominated WDMS binary from DR 8.
- SDSSJ100413.18+342950.8, a white dwarf plus (likely) late K star companion from DR 7.
- SDSSJ153648.31+010249.1, a white dwarf dominated WDMS binary from DR 7.
- SDSSJ220436.50-002313.7, a noisy spectrum of a WDMS binary from DR 7.

We add these five systems to our catalogue list. The total number of spectroscopic SDSS WDMS binaries thus raises to 2313 and the number of new DR 8 WDMS binaries increases to 47 (Table 4).

4.3 Comparison with Wei et al. (2013)

Wei et al. (2013) claim ~ 500 WDMS binaries in their list are not included in the catalogue by Rebassa-Mansergas et al. (2012a), suggesting that our algorithm has failed in identifying a large fraction of SDSS WDMS binaries. Here we investigate this issue in detail.

The first point to note is that out of the ~ 500 additional WDMS binaries identified by Wei et al. (2013), only 292 spectra of 281 individual objects have been made publicly available following the publication of their paper. The remaining ~ 200 systems are not longer considered WDMS binaries by the authors and have not been made available by them (Peng Wei & Ali Luo, private communication). We visually inspect the SDSS spectra and SDSS images of these 281 systems and find that only 85 of them are genuine WDMS binaries (see Table A3 for an updated classification of the remaining 196 objects), of which 40 are new identifications from spectroscopic plates observed as part of SDSS DR 8 (and therefore were of course not included in Rebassa-Mansergas et al. 2012a). The 45 remaining WDMS binaries were obtained on spectroscopic

Table 5. SDSS plate, modified Julian date (MJD) and fibre identifiers of 45 DR 7 WDMs binary spectra that are not included in the DR 7 WDMs binary catalogue by Rebassa-Mansergas et al. (2012a). These spectra were taken during observations performed for DR 7, however, made only publicly available within DR 8.

Object	plt	MJD	fib	Object	plt	MJD	fib	Object	plt	MJD	fib
SDSSJ002157.91-110331.6	1913	53295	242	SDSSJ102857.79+093129.9	2854	54465	576	SDSSJ155808.50+264225.8	2474	54333	598
SDSSJ011226.93+251149.8	2060	53388	274	SDSSJ104219.08+442916.0	2567	54179	636	SDSSJ161239.06+455132.3	814	5235	403
SDSSJ014143.68-093811.7	2865	54503	170	SDSSJ105346.29+291652.6	2359	53800	413	SDSSJ165112.44+415139.2	631	52054	474
SDSSJ030904.82-010100.9	412	51871	204	SDSSJ105421.97+512254.2	876	5234	533	SDSSJ171301.85+625135.9	352	51694	224
SDSSJ081716.98+054223.7	1296	52738	307	SDSSJ105617.52+505321.2	876	5234	590	SDSSJ171955.23+625106.8	352	51694	163
SDSSJ081959.21+060424.2	1296	52738	196	SDSSJ110750.15+050559.0	581	52353	495	SDSSJ172433.70+623410.0	352	51694	59
SDSSJ083410.38+135355.8	2427	53800	314	SDSSJ114312.57+000926.5	283	51660	437	SDSSJ172831.84+620426.5	352	51694	7
SDSSJ090455.46+184741.9	2285	53687	166	SDSSJ114312.57+000926.5	283	51584	433	SDSSJ173101.49+623316.0	352	51694	16
SDSSJ092737.67+255423.0	2294	54524	353	SDSSJ131334.74+023750.8	525	52029	509	SDSSJ173727.27+540352.2	360	51780	165
SDSSJ100529.93+521937.9	903	5238	169	SDSSJ132040.28+661214.8	496	51973	195	SDSSJ174214.72+541845.1	360	51780	115
SDSSJ100609.18+004417.1	269	51581	605	SDSSJ135930.96-101029.7	2716	54628	211	SDSSJ204117.50-062847.1	634	52149	47
SDSSJ101614.70+490930.4	873	5234	399	SDSSJ140723.04+003841.7	302	51616	464	SDSSJ222108.46+002927.7	1143	52592	462
SDSSJ101722.72+025147.8	574	52347	44	SDSSJ141220.70+654123.3	498	51973	545	SDSSJ222822.74+391239.8	2620	54339	73
SDSSJ101722.72+025147.8	574	52356	44	SDSSJ143746.70+573706.1	790	5234	120	SDSSJ224038.38-093541.4	722	52206	150
SDSSJ101722.72+025147.8	574	52366	50	SDSSJ150231.66+011046.0	310	51616	423	SDSSJ225334.79-090554.0	724	5223	433

plates that formally pre-date DR 8. In what follows we study these 45 DR 7 and 40 DR 8 WDMs binaries separately and compare them to the list of DR 7 WDMs binaries by Rebassa-Mansergas et al. (2012a) and the updated DR 8 WDMs binary catalogue presented in this work, respectively.

Comparing the details of the 45 DR 7 WDMs binaries with our DR 7 WDMs binary catalogue, we find only three systems that were not included in our list: SDSSJ083056.71+122546.6 (noisy spectrum of a WDMs binary), SDSSJ170014.24+242127.3 (a WDMs binary containing a hot white dwarf and an early-type M dwarf), and SDSSJ140127.24+484841.8 (noisy spectrum of a WDMs binary). The remaining 42 WDMs binaries that Wei et al. (2013) claim to be new identifications are in fact contained in our catalogue. However, Wei et al. (2013) analysed additional SDSS spectra (45, as two of the 42 objects have multiple SDSS spectroscopy) that were not part of the original DR 7 release, and hence were not available to us at the time of our analysis (Rebassa-Mansergas et al. 2012a). Those 45 spectra are not accessible via DR 7 web tools and the DR 7 casjobs data base, and appear only within DR 8. The modified Julian date, plate and fibre identifiers of these 45 WDMs binary spectra are provided in Table 5. The missed three objects and 45 WDMs binary spectra are added to our catalogue. The total number of spectroscopic SDSS WDMs binaries therefore increases to 2316 (Table 4)

We then compare the list of 40 DR 8 WDMs binaries from Wei et al. (2013) with the list of new DR 8 WDMs binaries presented in this work and find that all their listed objects (and spectra) are included in our catalogue.

5 CHARACTERIZATION OF THE SDSS DR 8 WDMs BINARY SAMPLE

As mentioned above, the spectroscopy within DR 8 focused on observing main sequence and red giant stars, following a different target selection compared to the earlier data releases. It is therefore expected that SDSS DR 8 WDMs bina-

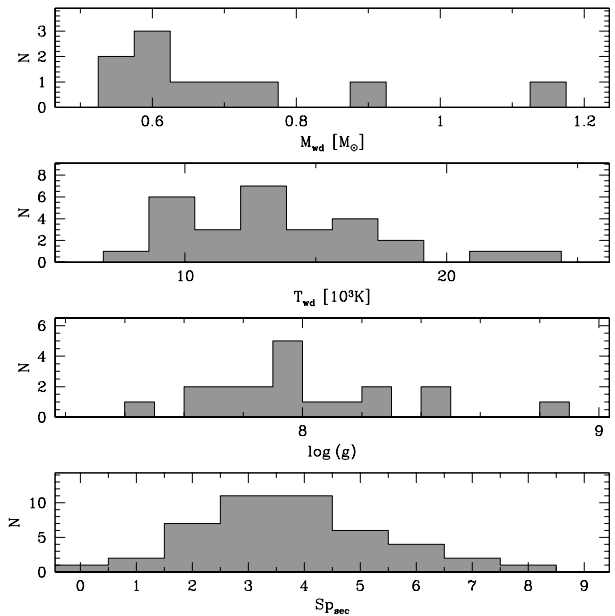


Figure 6. Distributions of white dwarf effective temperature, surface gravity and mass, and secondary star spectral type.

ries are drawn from a different parent population than those in our DR 7 catalogue (Rebassa-Mansergas et al. 2012a). To investigate this we obtained the stellar parameters of the new 47 DR 8 systems (Table 4)⁴.

We obtain the stellar parameters following the decomposition/fitting routine described by Rebassa-Mansergas et al. (2007). First, a given SDSS

⁴ For completeness, we also provide GALEX ultraviolet and UKIDSS infrared magnitudes, and measure the secondary star radial velocities for the new systems following the method described in Rebassa-Mansergas et al. (2008). This information has been added to our on-line data base of spectroscopic SDSS WDMs binaries, publicly available at <http://www.sdss-wdms.org>

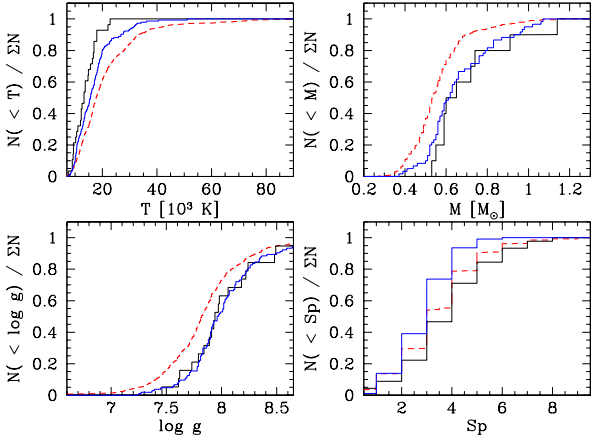


Figure 7. White dwarf effective temperature (top left), mass (top right), surface gravity (bottom left) and secondary star spectral type (bottom right) cumulative distributions of SDSS DR8 WDMS binaries (black solid lines) and of SDSS WDMS binaries from DR 7 (red dotted lines, excluding the SEGUE WDMS binary sample, represented as blue solid lines).

WDMS binary spectrum is fitted with a two-component model using a set of observed M dwarf and white dwarf templates. From the converged fit to each WDMS binary spectrum we record the spectral type of the secondary star. The best-fit M dwarf template, scaled by the appropriate flux scaling factor, is then subtracted and we fit the residual white dwarf spectrum with a model grid of DA white dwarfs (Koester 2010) to obtain the effective temperature and surface gravity. From a mass-radius relation for white dwarfs (Bergeron et al. 1995; Fontaine et al. 2001) we finally calculate the mass of the white dwarf.

For the following discussion we only consider white dwarf masses and gravities if the white dwarf temperature exceeds 12 000 K. This is due to a systematic increase in the surface gravity that has been observed in recent white dwarf spectroscopic studies below this value (Koester et al. 2009; Tremblay et al. 2011). In order to avoid contamination from unreliable stellar parameters, we additionally only consider objects with a relative error in the white dwarf parameters of less than 15 per cent. This results in 28, 19 and 10 WDMS binaries in the distributions of white dwarf effective temperatures, surface gravities and masses respectively, shown on the top panels of Figure 6. The spectral types of the secondary stars of 45 of our new systems are directly determined from the spectral template fitting and the corresponding distribution is provided on the bottom panel of Figure 6.

We compare the stellar parameter distribution of the new DR 8 WDMS binary sample with that of the DR 7 sample using Kolmogorov-Smirnov (KS) tests to the cumulative distributions in white dwarf effective temperature, surface gravity and mass, and we compare the spectral type distributions using a χ^2 test. In this exercise we separate the DR 7 catalogue into systems identified as part of our SEGUE survey for identifying systems containing cool white dwarfs (henceforth SEGUE WDMS binaries, Schreiber et al. 2007; Rebassa-Mansergas et al. 2012a), and stars observed as part

of the main SDSS program (henceforth Legacy WDMS binaries).

The comparison between the DR 8 and the Legacy WDMS binaries results in white dwarf parameter KS probabilities of $\lesssim 1$ per cent, and a secondary star spectral χ^2 probability of 99 per cent. The low KS probabilities found from the comparison of the cumulative distributions of the white dwarf parameters are not surprising and confirm that DR 8 WDMS binaries are drawn from a different parent population: whilst the distribution of secondary star spectral types is broadly similar between the DR 8 and Legacy WDMS binary samples, systematically cooler and more massive white dwarfs are found in the DR 8 sample (see Figure 7). By definition, our SEGUE survey targeted also WDMS binaries containing cool white dwarfs (and/or early-type secondaries, Section 1). It is therefore expected the SEGUE and DR 8 samples to be formed by similar white dwarf primary populations. This hypothesis is in agreement with the KS probabilities of white dwarf effective temperature, mass and surface gravity of 5, 76 and 96 per cent respectively (the secondary star spectral χ^2 probability is of 1 per cent). Note that the relatively low KS probability found from the comparison of the cumulative distributions of white dwarf effective temperatures is due to the white dwarf components of DR 8 WDMS binaries being systematically cooler than those in the SEGUE sample (top left panel of Figure 7). Given that WDMS binaries containing cool white dwarfs are under-represented in the current version of the SDSS WDMS binary catalogue, the 47 new discoveries within DR 8 represent an important addition to the spectroscopic sample.

6 SUMMARY

The current spectroscopic sample of SDSS WDMS binaries is strongly biased against systems containing cool white dwarfs and/or early type M dwarf companions. In this work we have provided a photometric sample of 3 419 SDSS WDMS binary candidates that has the potential of filling in this missing and important population. The success rate of detecting genuine WDMS binaries within our photometric candidates depends on the location in colour space and varies from 43 to 100 per cent, with an overall average of 84 per cent. The main contaminants are cataclysmic variables and quasars. We estimate that the majority (~ 70 per cent) of the selected WDMS binaries to contain white dwarfs with effective temperatures $\lesssim 10\,000$ – $15\,000$ K and secondary stars of spectral type $\sim M2$ – 3 .

We have also presented an updated version of the spectroscopic SDSS WDMS binary catalogue, which contains 2316 objects from DR 8. This is currently the largest and most homogeneous sample of spectroscopically identified compact binaries. We identify only a relatively small number, 47, of new WDMS binaries within the DR 8 spectroscopy. This is due to the bulk of DR 8 spectra being dominated by spectra of main sequence and giant stars. The sample of DR 8 WDMS binaries is clearly dominated by systems containing cool white dwarfs and therefore represents an important addition to the spectroscopic sample. Stellar parameters, magnitudes and secondary star radial velocities of the 47 new systems are obtained and made publicly avail-

able via our SDSS WDMS binary web site <http://www.sdss-wdms.org>.

ACKNOWLEDGMENTS

ARM acknowledges financial support from LAMOST fellowship and Fondecyt (3110049). MRS acknowledges support from Milenium Science Initiative, Chilean Ministry of Economy, Nucleus P10-022-F, and Fondecyt (1100782). The research leading to these results has received funding from the European Research Council under the European Union's Seventh Framework Programme (FP/2007-2013) / ERC Grant Agreement n. 267697 (WDTracer). BTG was supported in part by the UKs Science and Technology Facilities Council (ST/I001719/1).

REFERENCES

- Abazajian, K. N., et al., 2009, *ApJ*, 182, 543
 Adelman-McCarthy, J. K., et al., 2008, *ApJS*, 175, 297
 Aihara, H., et al., 2011, *ApJ*, 195, 26
 Badenes, C., van Kerkwijk, M. H., Kilic, M., Bickerton, S. J., Mazeh, T., Mullally, F., Tal-Or, L., Thompson, S. E., 2013, *MNRAS*, 429, 3596
 Bergeron, P., Wesemael, F., Beauchamp, A., 1995, *PASP*, 107, 1047
 Davis, P. J., Kolb, U., Willems, B., 2010, *MNRAS*, 403, 179
 Debes, J. H., Hoard, D. W., Wachter, S., Leisawitz, D. T., Cohen, M., 2011, *ApJ*, 197, 38
 Eisenstein, D. J., et al., 2011, *AJ*, 142, 72
 Farihi, J., Hoard, D. W., Wachter, S., 2010, *ApJ*, 190, 275
 Ferrario, L., 2012, *MNRAS*, 426, 2500
 Fontaine, G., Brassard, P., Bergeron, P., 2001, *PASP*, 113, 409
 Girven, J., Gänsicke, B. T., Steeghs, D., Koester, D., 2011, *MNRAS*, 417, 1210
 Heller, R., Homeier, D., Dreizler, S., Østensen, R., 2009, *A&A*, 496, 191
 Iben, I. J., Livio, M., 1993, *PASP*, 105, 1373
 Kleinman, S. J., et al., 2013, *ApJ*, 204, 5
 Koester, D., 2010, *Memorie della Societa Astronomica Italiana*, 81, 921
 Koester, D., Kepler, S. O., Kleinman, S. J., Nitta, A., 2009, *Journal of Physics Conference Series*, 172, 012006
 Lawrence, A., et al., 2007, *MNRAS*, 379, 1599
 Li, N., Thakar, A. R., 2008, *Computing in Science and Engineering*, 10, 18
 Liu, C., Li, L., Zhang, F., Zhang, Y., Jiang, D., Liu, J., 2012, *MNRAS*, 424, 1841
 Martin, D. C., et al., 2005, *ApJ Lett.*, 619, L1
 Miszalski, B., Acker, A., Moffat, A. F. J., Parker, Q. A., Udalski, A., 2009, *A&A*, 496, 813
 Morgan, D. P., West, A. A., Garcés, A., Catalán, S., Dhital, S., Fuchs, M., Silvestri, N. M., 2012, *AJ*, 144, 93
 Morrissey, P., et al., 2005, *ApJ*, 619, L7
 Nebot Gómez-Morán, A., et al., 2009, *A&A*, 495, 561
 Nebot Gómez-Morán, A., et al., 2011, *A&A*, 536, A43
 Parsons, S. G., Marsh, T. R., Copperwheat, C. M., Dhillon, V. S., Littlefair, S. P., Gänsicke, B. T., Hickman, R., 2010, *MNRAS*, 402, 2591
 Parsons, S. G., et al., 2012a, *MNRAS*, 420, 3281
 Parsons, S. G., et al., 2012b, *MNRAS*, 426, 1950
 Passy, J.-C., et al., 2012, *ApJ*, 744, 52
 Pyrzas, S., et al., 2009, *MNRAS*, 394, 978
 Pyrzas, S., et al., 2012, *MNRAS*, 419, 817
 Rebassa-Mansergas, A., Gänsicke, B. T., Rodríguez-Gil, P., Schreiber, M. R., Koester, D., 2007, *MNRAS*, 382, 1377
 Rebassa-Mansergas, A., Gänsicke, B. T., Schreiber, M. R., Koester, D., Rodríguez-Gil, P., 2010, *MNRAS*, 402, 620
 Rebassa-Mansergas, A., Nebot Gómez-Morán, A., Schreiber, M. R., Girven, J., Gänsicke, B. T., 2011, *MNRAS*, 413, 1121
 Rebassa-Mansergas, A., Nebot Gómez-Morán, A., Schreiber, M. R., Gänsicke, B. T., Schwöpe, A., Gallardo, J., Koester, D., 2012a, *MNRAS*, 419, 806
 Rebassa-Mansergas, A., Schreiber, M. R., Gänsicke, B. T., 2013, *MNRAS*, 429, 3570
 Rebassa-Mansergas, A., et al., 2008, *MNRAS*, 390, 1635
 Rebassa-Mansergas, A., et al., 2012b, *MNRAS*, 423, 320
 Ricker, P. M., Taam, R. E., 2012, *ApJ*, 746, 74
 Schneider, D. P., et al., 2010, *VizieR Online Data Catalog*, 7260, 0
 Schreiber, M. R., Gänsicke, B. T., 2003, *A&A*, 406, 305
 Schreiber, M. R., Nebot Gomez-Moran, A., Schwöpe, A. D., 2007, in R. Napiwotzki & M. R. Burleigh, ed., 15th European Workshop on White Dwarfs, vol. 372 of *Astronomical Society of the Pacific Conference Series*, p. 459
 Schreiber, M. R., Gänsicke, B. T., Southworth, J., Schwöpe, A. D., Koester, D., 2008, *A&A*, 484, 441
 Schreiber, M. R., et al., 2010, *A&A*, 513, L7+
 Seibert, M., et al., 2012, in American Astronomical Society Meeting Abstracts 219, vol. 219 of *American Astronomical Society Meeting Abstracts*, p. 340.01
 Silvestri, N. M., et al., 2006, *AJ*, 131, 1674
 Skrutskie, M. F., et al., 2006, *AJ*, 131, 1163
 Smolčić, V., et al., 2004, *ApJ*, 615, L141
 Steele, P. R., et al., 2013, *MNRAS*, 429, 3492
 Stoughton, C., et al., 2002, *AJ*, 123, 485
 Tappert, C., Gänsicke, B. T., Rebassa-Mansergas, A., Schmidtobreick, L., Schreiber, M. R., 2011, *A&A*, 531, A113
 Tremblay, P.-E., Ludwig, H.-G., Steffen, M., Bergeron, P., Freytag, B., 2011, *A&A*, 531, L19
 Warren, S. J., et al., 2007, *MNRAS*, 375, 213
 Webbink, R. F., 2008, in E. F. Milone, D. A. Leahy, & D. W. Hobill, ed., *Astrophysics and Space Science Library*, vol. 352 of *Astrophysics and Space Science Library*, p. 233
 Wei, P., et al., 2013, *MNRAS*, 431, 1800
 Willems, B., Kolb, U., 2004, *A&A*, 419, 1057
 Wright, E. L., et al., 2010, *AJ*, 140, 1868
 Yanny, B., et al., 2009, *AJ*, 137, 4377
 York, D. G., et al., 2000, *AJ*, 120, 1579
 Zorotovic, M., Schreiber, M. R., Gänsicke, B. T., Nebot Gómez-Morán, A., 2010, *A&A*, 520, A86

APPENDIX A: TABLES

Table A1. 28 systems in the list by Liu et al. (2012) are not considered WDMS binaries due to morphological problems in their SDSS images and/or by visual inspection of the SDSS spectra. We provide here a revised classification for these systems.

Object	class.	Object	class.
SDSSJ001324.33-085021.4	unknown	SDSSJ113722.24+014858.5	CV
SDSSJ073721.36+464136.9	MS+MS sup.	SDSSJ114955.70+284507.3	CV
SDSSJ073914.18+331611.5	MS+MS sup.	SDSSJ122740.82+513925.0	CV
SDSSJ082619.17+110852.7	WD	SDSSJ131119.61-010420.5	MS+MS sup.
SDSSJ083751.00+383012.5	unknown	SDSSJ132125.64+051236.4	M star
SDSSJ083814.59+484134.9	MS+MS sup.	SDSSJ132151.51+420014.1	M star+gal.
SDSSJ084008.35+490337.9	unknown	SDSSJ141921.58+020710.2	MS+MS sup.
SDSSJ091242.18+620940.1	CV	SDSSJ145314.93+015121.9	M star
SDSSJ092219.55+421256.8	CV	SDSSJ154311.83+101722.2	MS+MS sup.
SDSSJ094636.60+444644.7	CV	SDSSJ154932.60+003524.3	MS+MS sup.
SDSSJ100614.12+101620.7	MS+MS sup.	SDSSJ155707.60+031813.8	MS+MS sup.
SDSSJ103934.07+602744.9	WD	SDSSJ162520.29+120308.8	CV
SDSSJ105547.89+034555.1	MS+MS sup.	SDSSJ222156.96-005118.1	MS+MS sup.
SDSSJ111544.56+425822.4	CV	SDSSJ235356.45-110554.2	MS+MS sup.

Table A2. 80 systems in the list by Morgan et al. (2012) are not considered WDMS binaries due to morphological problems in their SDSS images and/or by visual inspection of the SDSS spectra. We provide here a revised classification for these systems.

Object	class.	Object	class.	Object	class.
SDSSJ001831.02-093139.1	MS+MS sup.	SDSSJ093859.24+020925.2	QSO+M star	SDSSJ152930.91+032754.0	M star+galaxy
SDSSJ004517.26+150949.1	MS+MS sup.	SDSSJ094716.59+675402.6	morph. problems	SDSSJ153041.18-012008.2	MS+MS sup.
SDSSJ005827.25+005642.6	MS+MS sup.	SDSSJ100844.74+120710.3	MS+MS sup.	SDSSJ160349.69+084935.8	MS+MS sup.
SDSSJ010338.92+142538.6	MS+MS sup.	SDSSJ102252.04+275828.9	MS+MS sup.	SDSSJ161338.34+112740.1	MS+MS sup.
SDSSJ012839.69-004223.4	MS+MS sup.	SDSSJ103224.99+542915.4	MS+MS sup.	SDSSJ161352.75+363356.1	MS+MS sup.
SDSSJ014349.22+002130.1	QSO+M star	SDSSJ110213.46+553939.4	noisy	SDSSJ161631.18+050936.2	MS+MS sup.
SDSSJ020538.10+005835.3	MS+MS sup.	SDSSJ111358.28+203206.1	MS+MS sup.	SDSSJ162520.30+120308.8	CV
SDSSJ031209.19+004701.6	MS+MS sup.	SDSSJ111544.56+425822.4	CV	SDSSJ162517.58+140134.6	MS+MS sup.
SDSSJ032131.02+000617.3	MS+MS sup.	SDSSJ114036.04+575743.4	MS+MS sup.	SDSSJ162702.51+252235.9	MS+MS sup.
SDSSJ033131.33+005149.1	MS+MS sup.	SDSSJ114524.45-020938.2	MS+MS sup.	SDSSJ165932.19+422708.4	MS+MS sup.
SDSSJ033436.72+005853.7	MS+MS sup.	SDSSJ114653.68+012518.2	MS+MS sup.	SDSSJ170112.29+193819.1	MS+MS sup.
SDSSJ053135.46-002713.3	MS+MS sup.	SDSSJ125341.55+555322.4	MS+MS sup.	SDSSJ170357.74+401500.5	MS+MS sup.
SDSSJ053233.12-001148.5	MS+MS sup.	SDSSJ125324.57+555457.4	MS+MS sup.	SDSSJ185808.92+192742.2	MS+MS sup.
SDSSJ053206.23-001220.6	MS+MS sup.	SDSSJ130942.34+383054.0	MS+MS sup.	SDSSJ204001.99-003132.9	MS+MS sup.
SDSSJ064941.01+290132.6	MS+MS sup.	SDSSJ131227.94+161505.3	field WD + field M star	SDSSJ204720.07-003221.8	MS+MS sup.
SDSSJ065012.35+273950.0	MS+MS sup.	SDSSJ131954.58-011208.3	MS+MS sup.	SDSSJ205732.78+010617.3	MS+MS sup.
SDSSJ072528.10+384011.1	MS+MS sup.	SDSSJ133645.56-002231.3	MS+MS sup.	SDSSJ205730.72-005346.3	MS+MS sup.
SDSSJ073531.86+315015.3	MS+MS sup.	SDSSJ134554.22+005221.0	MS+MS sup.	SDSSJ205857.10-075440.6	no spectrum
SDSSJ080329.47+361934.5	WD+red source	SDSSJ140236.66+542145.5	morph. problems	SDSSJ210616.52-062743.3	MS+MS sup.
SDSSJ080657.22+544546.5	no spectrum	SDSSJ141325.11+515017.0	MS+MS sup.	SDSSJ221410.63-002756.3	MS+MS sup.
SDSSJ081228.68+323533.1	unknown	SDSSJ143654.58-010515.4	MS+MS sup.	SDSSJ222130.45+001801.8	QSO+M star
SDSSJ081600.20+431339.2	no spectrum	SDSSJ143717.41+385626.8	morph. problems	SDSSJ222944.28+011323.4	MS+MS sup.
SDSSJ083437.99+443349.4	MS+MS sup.	SDSSJ144821.54+433516.9	MS+MS sup.	SDSSJ223223.76+135434.5	QSO+M star
SDSSJ083552.05+143031.7	MS+MS sup.	SDSSJ145814.81+001242.7	noisy	SDSSJ233227.56+531041.5	MS+MS sup.
SDSSJ083711.50+093828.9	morph. problems	SDSSJ151923.51+073403.7	MS+MS sup.	SDSSJ223530.61-000536.0	morph. problems
SDSSJ084225.23+174453.8	MS+MS sup.	SDSSJ152244.22+072945.4	MS+MS sup.	SDSSJ223520.74-000558.1	no spectrum
SDSSJ084344.93+262000.7	MS+MS sup.			SDSSJ234456.89+010757.8	MS+MS sup.

Table A3. 196 systems in the list by Wei et al. (2013) are not considered WDMS binaries due to morphological problems in their SDSS images and/or by visual inspection of the SDSS spectra. We provide here a revised classification for these systems.

Object	class.	Object	class.	Object	class.
SDSSJ000421.61+004341.6	noisy M star	SDSSJ082555.66+433526.4	MS+MS sup.	SDSSJ143920.72+445014.5	unknown
SDSSJ001258.85+005920.7	MS+MS sup.	SDSSJ083055.38+062554.0	MS+MS sup.	SDSSJ144455.91+503622.4	MS+MS sup.
SDSSJ001322.94+151457.7	morph. problems	SDSSJ083202.01+124223.4	MS+MS sup.	SDSSJ145758.26-005549.5	morph. problems
SDSSJ001324.33-085021.4	MS+MS sup.	SDSSJ083711.50+093828.9	morph. problems	SDSSJ150916.11+094227.0	MS+MS sup.
SDSSJ001601.40+000832.4	MS+MS sup.	SDSSJ083751.00+383012.5	unknown	SDSSJ151923.51+073403.7	MS+MS sup.
SDSSJ001610.17-002421.6	MS+MS sup.	SDSSJ084224.78+023907.1	MS+MS sup.	SDSSJ152244.22+072945.4	MS+MS sup.
SDSSJ001658.16-101108.4	MS+MS sup.	SDSSJ084225.23+174453.8	MS+MS sup.	SDSSJ152458.89+585131.5	morph. problems
SDSSJ002334.83+004021.9	MS+MS sup.	SDSSJ084324.98+104110.7	MS+MS sup.	SDSSJ153119.09-023008.0	MS+MS sup.
SDSSJ004517.26+150949.1	morph. problems	SDSSJ084344.93+262000.7	MS+MS sup.	SDSSJ153238.96+003435.2	MS+MS sup.
SDSSJ005444.02-002120.1	MS+MS sup.	SDSSJ085057.18+381941.7	MS+MS sup.	SDSSJ153243.35+312057.3	morph. problems
SDSSJ005827.25+005642.6	MS+MS sup.	SDSSJ090155.27+123710.7	MS+MS sup.	SDSSJ153350.13-011007.2	MS+MS sup.
SDSSJ011248.52+001132.2	unknown	SDSSJ090323.57+470406.9	morph. problems	SDSSJ153434.40+023801.2	MS+MS sup.
SDSSJ012127.23-092905.0	M star + back.	SDSSJ090848.27+335354.8	morph. problems	SDSSJ153453.47+263238.7	morph. problems
SDSSJ012839.69-004223.4	MS+MS sup.	SDSSJ091242.18+620940.1	CV	SDSSJ154544.60+094823.9	MS+MS sup.
SDSSJ013701.06-091234.9	CV	SDSSJ093919.09+274314.0	WD	SDSSJ154653.68+573533.8	MS+MS sup.
SDSSJ015151.87+140047.2	CV	SDSSJ094056.07+095408.6	morph. problems	SDSSJ155156.59+352928.1	MS+MS sup.
SDSSJ020357.55-005424.6	MS+MS sup.	SDSSJ094636.60+444644.8	CV	SDSSJ155349.21+394106.2	unknown
SDSSJ020605.67-001723.7	MS+MS sup.	SDSSJ095228.57+540340.0	morph. problems	SDSSJ155412.34+272152.4	CV
SDSSJ021041.54-001739.2	noisy M star	SDSSJ095306.14+250905.5	MS+MS sup.	SDSSJ155644.24-000950.2	CV
SDSSJ025448.73+002310.6	MS+MS sup.	SDSSJ100614.12+101620.7	MS+MS sup.	SDSSJ160349.69+084935.8	MS+MS sup.
SDSSJ034538.00-064326.2	morph. problems	SDSSJ103738.28-002328.9	MS+MS sup.	SDSSJ160420.96+512734.5	MS+MS sup.
SDSSJ025750.13-002757.3	MS+MS sup.	SDSSJ100904.57+114630.8	M star + blue excess	SDSSJ160839.59+450358.5	morph. problems
SDSSJ030534.15+385308.0	morph. problems	SDSSJ102329.04+092926.1	broken spectrum	SDSSJ160941.64+525332.7	MS+MS sup.
SDSSJ030739.91+003656.0	MS+MS sup.	SDSSJ103110.75+425709.9	MS+MS sup.	SDSSJ162517.58+140134.6	morph. problems
SDSSJ031104.85+412109.4	MS+MS sup.	SDSSJ103301.59+091757.2	morph. problems	SDSSJ162520.30+120308.8	CV
SDSSJ033131.33+005149.1	MS+MS sup.	SDSSJ103623.24+081007.0	morph. problems	SDSSJ162702.51+252235.9	MS+MS sup.
SDSSJ034538.00-064326.2	M star + galaxy	SDSSJ103738.28-002328.9	MS+MS sup.	SDSSJ162803.71+165855.8	MS+MS sup.
SDSSJ044403.97-054659.9	MS+MS sup.	SDSSJ104730.07+605457.4	WD	SDSSJ163809.60+453308.6	noisy M star
SDSSJ045325.66-054459.1	MS+MS sup.	SDSSJ105018.43+423406.3	MS+MS sup.	SDSSJ165343.40+630549.3	morph. problems
SDSSJ053125.11-001850.8	morph. problems	SDSSJ105420.35+163154.6	MS+MS sup.	SDSSJ170053.30+400357.6	unknown
SDSSJ053135.46-002713.3	noisy M star	SDSSJ105707.25+261416.7	active M star	SDSSJ170112.29+193819.1	MS+MS sup.
SDSSJ053201.53-002916.1	M star + blue excess	SDSSJ110330.10+323236.0	M star + galaxy	SDSSJ170213.26+322954.1	CV
SDSSJ053206.23-001220.6	morph. problems	SDSSJ110555.86-165634.4	MS+MS sup.	SDSSJ170259.78-201609.2	MS+MS sup.
SDSSJ053233.12-001148.5	M star + blue excess	SDSSJ111358.28+203206.1	morph. problems	SDSSJ170919.90+612016.8	morph. problems
SDSSJ053515.70-011050.9	M star	SDSSJ111544.56+425822.4	CV	SDSSJ172943.51+330220.2	MS+MS sup.
SDSSJ053528.67-011414.7	M star + blue excess	SDSSJ113722.25+014858.6	CV	SDSSJ174014.75+551157.9	MS+MS sup.
SDSSJ053530.27-010720.6	M star + blue excess	SDSSJ114036.04+575743.5	morph. problems	SDSSJ191404.82+781725.3	MS+MS sup.
SDSSJ053617.85-005507.1	M star	SDSSJ120544.40+614103.9	MS+MS sup.	SDSSJ191956.88+382900.4	MS+MS sup.
SDSSJ053619.98-010107.0	M star + blue excess	SDSSJ120756.53+032356.3	MS+MS sup.	SDSSJ192840.06+792244.7	MS+MS sup.
SDSSJ053639.15-005905.2	M star	SDSSJ121226.69+252158.4	MS+MS sup.	SDSSJ193822.75+621212.3	noisy M star
SDSSJ053806.74-010817.8	active M star	SDSSJ122454.76+125212.4	morph. problems	SDSSJ200942.51-125234.9	MS+MS sup.
SDSSJ060910.64+241858.5	morph. problems	SDSSJ123032.23+042838.2	MS+MS sup.	SDSSJ201808.19+754654.7	MS+MS sup.
SDSSJ065056.13+164319.9	morph. problems	SDSSJ123932.01+210806.3	unknown	SDSSJ203708.43+151909.1	MS+MS sup.
SDSSJ070105.84+292941.9	MS+MS sup.	SDSSJ124240.71+135540.7	early type star	SDSSJ204322.39-003104.4	noisy M star
SDSSJ072528.10+384011.1	unknown	SDSSJ124548.48+231346.7	morph. problems	SDSSJ210616.52-062743.3	MS+MS sup.
SDSSJ072918.08+414138.0	MS+MS sup.	SDSSJ125324.57+555457.4	morph. problems	SDSSJ211748.66+115406.9	MS+MS sup.
SDSSJ073430.01+314013.7	morph. problems	SDSSJ125341.55+555322.4	morph. problems	SDSSJ213327.56-000929.5	MS+MS sup.
SDSSJ073442.76+314449.3	morph. problems	SDSSJ125526.05+381438.0	MS+MS sup.	SDSSJ214854.81-070300.9	MS+MS sup.
SDSSJ073447.51+314510.0	morph. problems	SDSSJ125526.45+381656.5	morph. problems	SDSSJ215457.67-000120.0	MS+MS sup.
SDSSJ073531.86+315015.3	MS+MS sup.	SDSSJ125918.24+235632.7	MS+MS sup.	SDSSJ215503.22-010045.3	noisy M star
SDSSJ073721.35+464136.9	MS+MS sup.	SDSSJ130942.34+383054.0	morph. problems	SDSSJ220447.19-005324.8	morph. problems
SDSSJ074505.56+315054.9	MS+MS sup.	SDSSJ131954.58-011208.3	MS+MS sup.	SDSSJ221410.59-002754.5	MS+MS sup.
SDSSJ075117.10+144423.6	M star + blue excess	SDSSJ132517.49+550020.3	morph. problems	SDSSJ221949.37+005731.2	WD
SDSSJ075227.56+182957.5	MS+MS sup.	SDSSJ132935.64-022711.9	MS+MS sup.	SDSSJ223520.74-000558.1	morph. problems
SDSSJ075339.62+353213.2	unknown	SDSSJ133841.30+101602.2	unknown	SDSSJ223530.61-000536.0	morph. problems
SDSSJ075465.51+394754.6	noisy M star	SDSSJ134159.10+041224.0	MS+MS sup.	SDSSJ225703.39-010457.8	MS+MS sup.
SDSSJ075605.79+664505.5	MS+MS sup.	SDSSJ134748.79+235153.0	MS+MS sup.	SDSSJ230949.12+213516.7	active M star
SDSSJ075633.87+355534.2	MS+MS sup.	SDSSJ135554.18+070822.5	MS+MS sup.	SDSSJ231808.91-091145.3	morph. problems
SDSSJ075732.50+243024.2	MS+MS sup.	SDSSJ140405.76+641507.6	unknown	SDSSJ232237.76+135859.2	MS+MS sup.
SDSSJ080045.22+402318.5	WD	SDSSJ140550.20+231113.4	unknown	SDSSJ232753.44+133855.5	MS+MS sup.
SDSSJ080104.16+391320.9	MS+MS sup.	SDSSJ140550.31+641947.0	unknown	SDSSJ233010.65+535854.4	MS+MS sup.
SDSSJ080140.00+250617.0	morph. problems	SDSSJ141325.11+515017.1	morph. problems	SDSSJ233227.37+531051.5	morph. problems
SDSSJ080237.16+134909.5	noisy M star	SDSSJ141710.11+103415.8	M star + galaxy	SDSSJ234339.71-004852.5	MS+MS sup.
SDSSJ080329.47+361934.5	morph. problems	SDSSJ142830.48+013443.6	MS+MS sup.	SDSSJ234811.79+140926.4	G star
SDSSJ081245.00+293500.0	MS+MS sup.	SDSSJ143332.31+414117.0	MS+MS sup.		